Support Information

Improving Surface Adsorption *via* Shape Control of Hematite α-Fe_2O_3 Nanoparticle for Sensitive Dopamine Sensors

Anran Chen[†], Liang Xu[†], Xiaojing Zhang[†], Zhimao Yang[†,‡], Shengchun Yang[*,†,‡]

[†]School of Science, MOE Key Laboratory for Nonequilibrium Synthesis and Modulation of Condensed Matter, State Key Laboratory for Mechanical Behavior of Materials, Xi'an Jiaotong University, Xi'an, Shaanxi 710049, People's Republic of China.

[‡]Collaborative Innovation Center of Suzhou Nano Science and Technology, Suzhou Academy of Xi'an Jiaotong University, 215000, Suzhou, People's Republic of China.

*Corresponding Author

Prof. Dr. Shengchun Yang, E-mail: ysch1209@mail.xjtu.edu.cn. Phone: +86-29-82663034.

Table S1. Summary of Synthetic Parameters for the Four Kinds of α-Fe_2O_3 Nanoparticles

sample	$Fe(NO_3)_3 \cdot 9H_2O$ (g)	KOH (g)	ethylene glycol (mL)	distilled water (mL)	ethanol (mL)	T (°C)	holding time (h)	stirring treatment
Shuttle Fe_2O_3	0.2425	0.123	6	12	2	200	8	applied
Pseudo-shuttle Fe_2O_3	0.2425	0.123	6	10	4	200	8	applied
Polyhedron Fe_2O_3	0.2425	0.123	6	6	8	200	8	applied
Drum Fe_2O_3	0.2425	0.123	6	4	10	200	8	applied

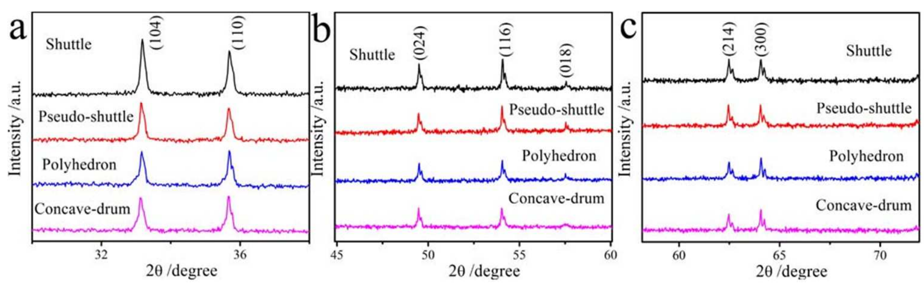

Figure S1. XRD patterns of the as-prepared shuttle, pseudo-shuttle, polyhedron and drum α-Fe_2O_3 NPs; (a-c) Enlarged region around the (104)/(110), (024)/(116) and (214)/(300) diffraction peaks of the four samples.

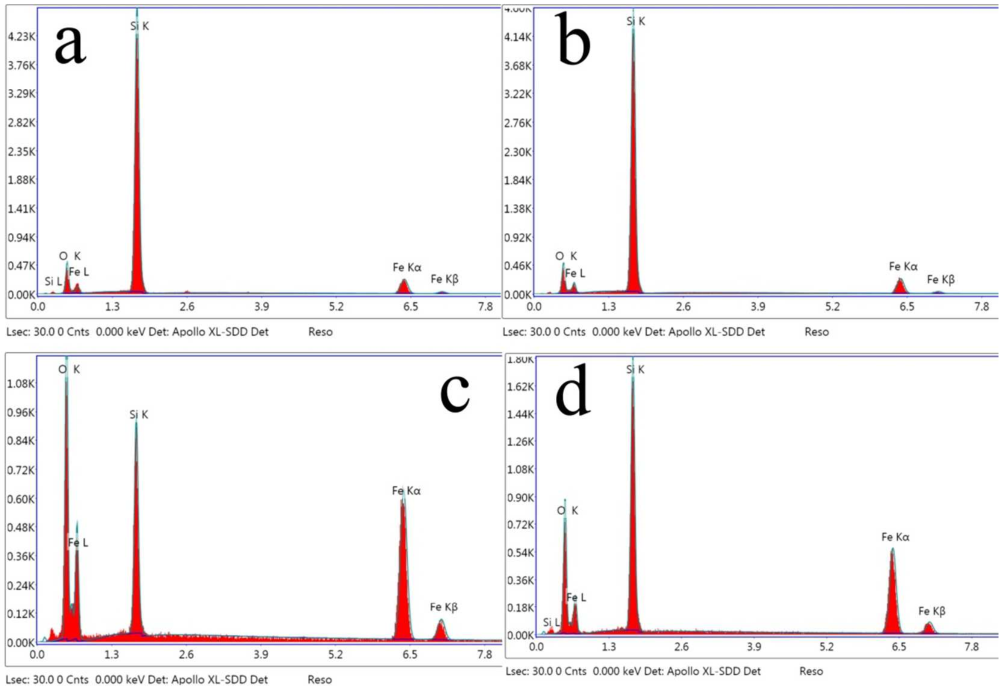

Figure S2. EDAX spectra of the as-prepared shuttle, pseudo-shuttle, polyhedron and drum α-Fe_2O_3 NPs (a-d).

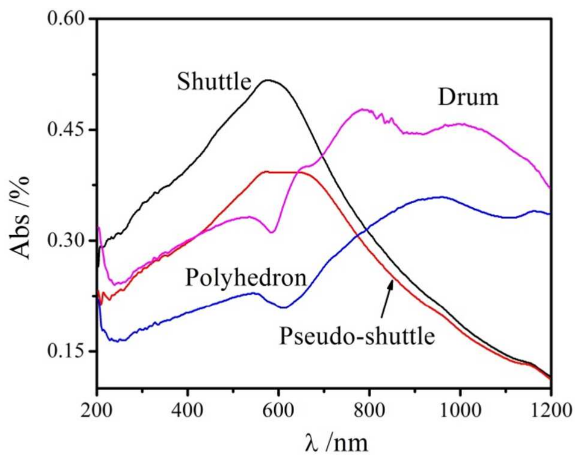

Figure S3. UV/Vis spectra of the all α-Fe_2O_3 NPs dispersed in water.

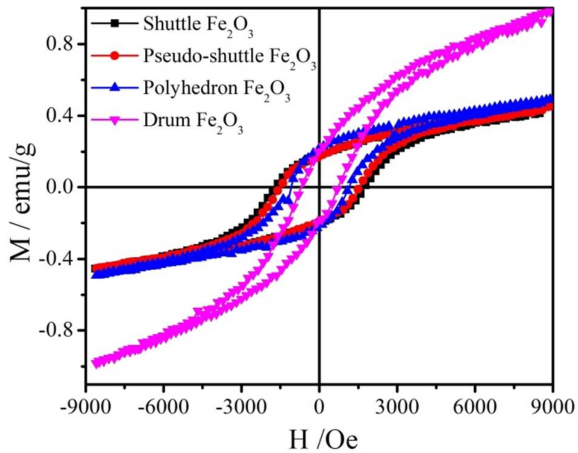

Figure S4. Magnetic hysteresis loops of the as-prepared shuttle, pseudo-shuttle, polyhedron and drum α-Fe_2O_3 NPs.

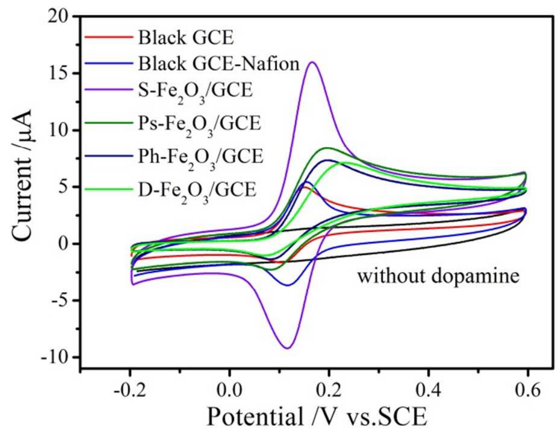

Figure S5. Typical cyclic voltammograms measured with and without 0.2 mM DA use S-Fe_2O_3/GCE, Ps-Fe_2O_3/GCE, Ph-Fe_2O_3/GCE, D-Fe_2O_3/GCE, black GCE (without 10 μL Nafion solution) and black GCE-Nafion (with 10 μL Nafion solution) in the phosphate buffer solution (PBS, pH 7.0). Scan rate: 50 mVs^{-1}.

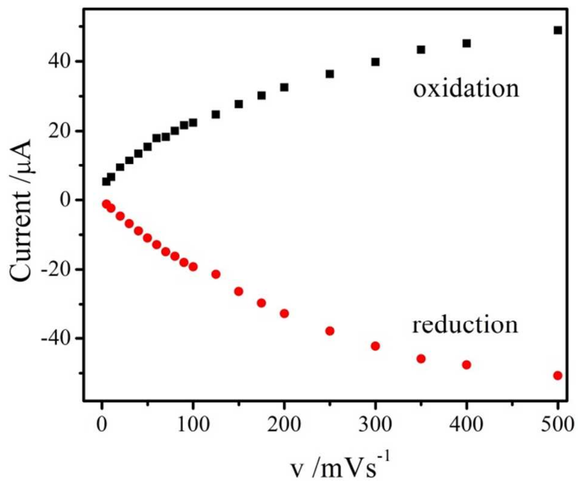

Figure S6. The dependency of anodic and cathodic peak currents to the potential sweep rate.

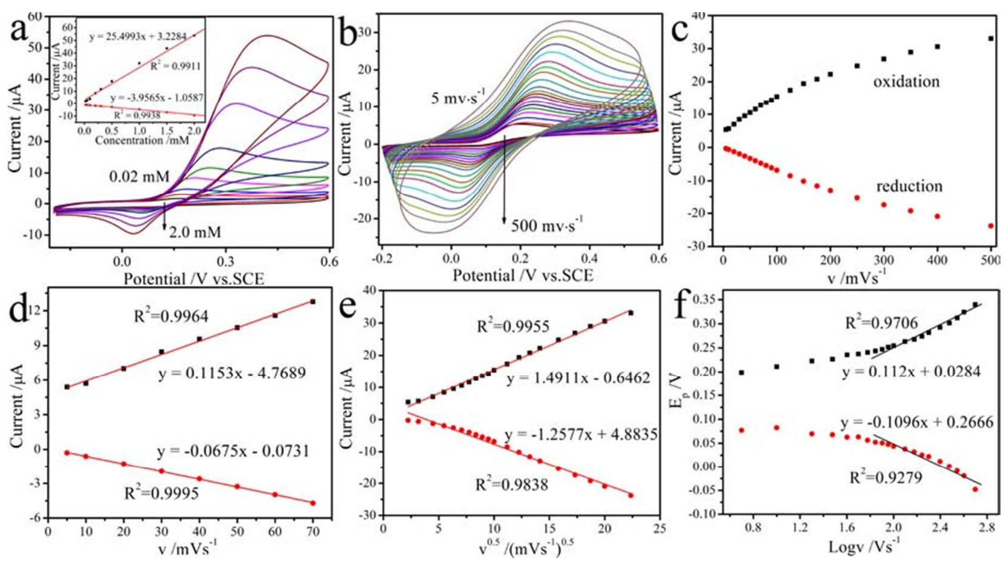

Figure S7. (a) Typical cyclic voltammograms of Ps-Fe_2O_3/GCE in the presence of different concentrations of DA in a PBS solution (pH 7.0). (b) Typical cyclic voltammograms of Ps-Fe_2O_3/GCE in PBS solution (pH 7.0, containing 0.2 mM DA) at different potential sweep rates of 5 to 500 mVs^{-1}. (c) The dependency of anodic and cathodic peak currents to the potential sweep rate. Proportionality of anodic and cathodic peak currents to the linear relation (d) and square root of potential sweep rate (e). (f) The dependency of peak potential vs. Logarithm of scan rates.

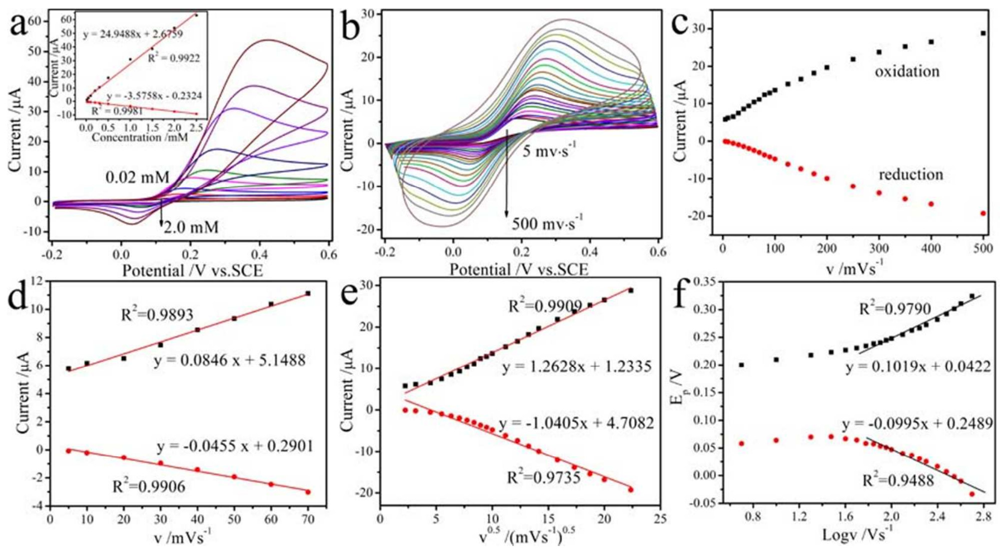

FigureS8. Typical cyclic voltammograms of Ph-Fe_2O_3/GCE in the presence of different concentrations of DA in a PBS solution (pH 7.0). (b) Typical cyclic voltammograms of Ph-Fe_2O_3/GCE in PBS solution (pH 7.0, containing 0.2 mM DA) at different potential sweep rates of 5 to 500 mVs^{-1}. (c) The dependency of anodic and cathodic peak currents to the potential sweep rate. Proportionality of anodic and cathodic peak currents to the linear relation (d) and square root of potential sweep rate (e). (f) The dependency of peak potential vs. Logarithm of scan rates.

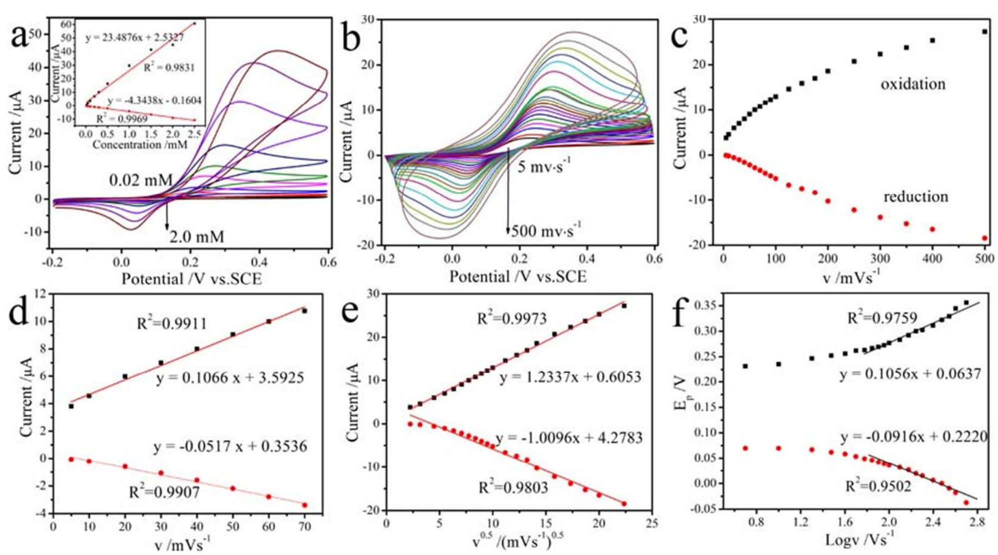

Figure S9. Typical cyclic voltammograms of D-Fe_2O_3/GCE in the presence of different concentrations of DA in a PBS solution (pH 7.0). (b) Typical cyclic voltammograms of D-Fe_2O_3/GCE in PBS solution (pH 7.0, containing 0.2 mM DA) at different potential sweep rates of 5 to 500 mVs^{-1}. (c) The dependency of anodic and cathodic peak currents to the potential sweep rate. Proportionality of anodic and cathodic peak currents to the linear relation (d) and square root of potential sweep rate (e). (f) The dependency of peak potential vs. Logarithm of scan rates.

Table S2. Summary of Electrochemistry Parameters for the Four Kinds α-Fe_2O_3 Nanoparticles

Sample	Concentration		Scan rate v <60 mVs^{-1}		Scan rate v >70 mVs^{-1}		n	α	k_s	Γ /10^{-5}
	k_1	k_2	k'_1	k'_2	k''_1	k''_2				
S-Fe_2O_3	28.307	-18.045	0.2259	-0.2129	2.2861	-2.7470	0.9649	0.6346	0.2000	1.81
Ps-Fe_2O_3	25.499	-3.957	0.1153	-0.0675	1.4911	-1.2577	1.0667	0.5054	0.2808	1.01
Ph-Fe_2O_3	24.949	-3.576	0.0846	-0.0455	1.2628	-1.0405	1.1736	0.5059	0.2743	0.74
D-Fe_2O_3	23.488	-4.344	0.1066	-0.0517	1.2337	-1.0096	1.2047	0.5355	0.1656	0.68

Note:
k1: the slope of oxidation current of cyclic voltammograms in the presence of different concentrations of dopamine.
k2: the slope of reduction current of cyclic voltammograms in the presence of different concentrations of dopamine.
k'1: the slope of linear equation of anodic peak currents vs. scan rate.
k'2: the slope of linear equation of cathodic peak currents vs. scan rate.
k''1: the slope of proportionality of anodic peak currents to square root of potential sweep rate.
k''2: the slope of proportionality of cathodic peak currents to square root of potential sweep rate.
n: the number of electrons transferred.
α: transfer coefficient.
ks: electron transfer rate constant.
Γ: electrochemical active surface area of the electrode.

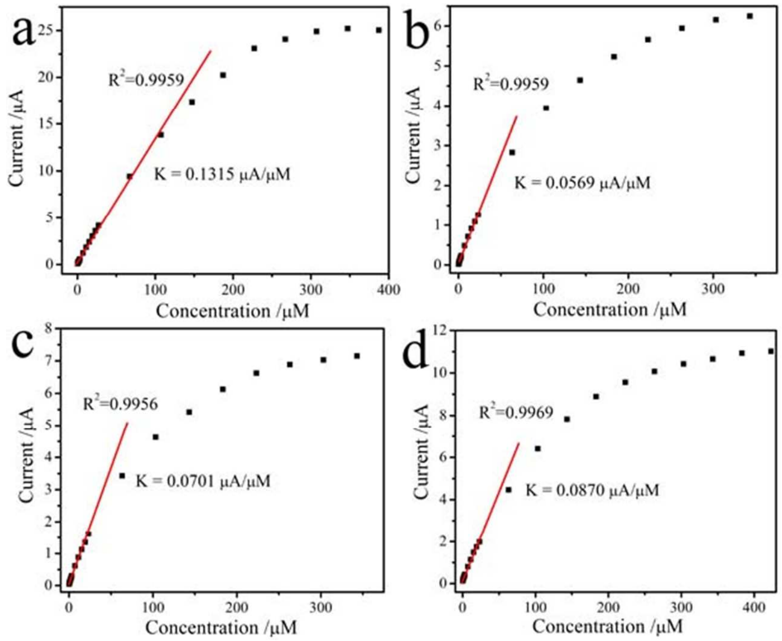

Figure S10. Corresponding calibration curve of the S-Fe_2O_3/GCE (a), Ps-Fe_2O_3/GCE (b), Ph-Fe_2O_3/GCE (c), D-Fe_2O_3/GCE (d) with successive addition of dopamine at regular intervals.

Table S3. Summary of Electrochemistry Parameters of Amperometric Responses for the Four Kinds α-Fe_2O_3 Nanoparticles

	Linear range μM	Slope $\mu A \mu M^{-1}$	Adj.R^2	Sensitivity $\mu A\ mM^{-1}\ cm^{-2}$	Detection limit nM
S-Fe_2O_3	0.2-107.2	0.1315	0.9959	671.0204	31.25
Ps-Fe_2O_3	0.2-23.2	0.0569	0.9947	290.3061	72.23
Ph-Fe_2O_3	0.2-23.2	0.0701	0.9956	357.6531	58.63
D-Fe_2O_3	0.2-23.2	0.0870	0.9969	443.8776	47.24

Note:
Slope: the slope of linear equation of amperometric response.
Adj.R^2: linear correlation coefficient.

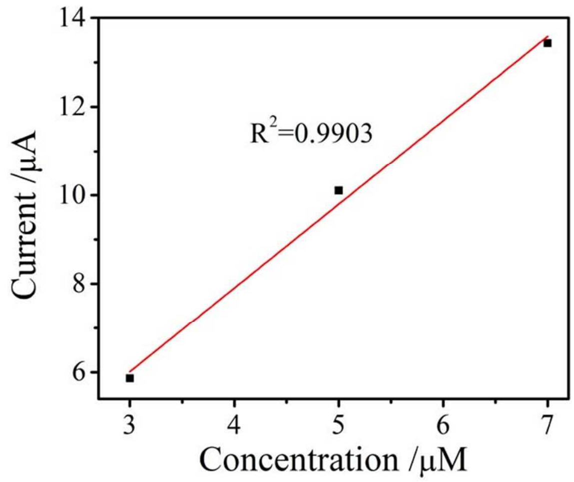

Figure S11. The corresponding calibration curve of currents by addition of DA in the presence of different interfering substance in a PBS solution (pH 7.0).

Table S4. Comparison of analytical performance of various dopamine biosensors

Dopamine biosensore	Method	Sensitivity ($\mu AmM^{-1}cm^{-2}$)	Linear range (μM)	Detection limit (nM)	Response time (s)	Reference
CNPEs	Fast-scan Cyclic voltammetry (FSCV)	Not given	0.1 - 10	25	Not given	Rees et al.,[1] 2015
NSG-Fe_2O_3	CA	411.69	0.3 - 210	35	Not given	Yasmin et al.,[2]
ERGO-DA	CA	142.89	0.5 - 100	40	> 10	Han et al.,[3]
Fe_3O_4@GNs/Nafion	DPV	Not given	0.02 - 130	7	Not given	Zhang et al.,[4]
Fe_3O_4@Au-S-Fc/GS -chitosan	DPV	Not given	0.5 - 50	100	Not given	Liu et al.,[5]
PEDOT/RGO	CA	Not given	0.1 - 175	39	Not given	Wang et al.,[6]
GO/SiO_2-MIPs	CA	Not given	0.05 - 160	30	Not given	Zeng et al.,[7]
TENS	Triboelectric nanogenerator	Not given	10 - 1000	500	Not given	Jie et al.,[8]
$Au_{70}Pt_{30}$	DPV	17.83	0.5 - 20	51	Not given	Oko et al.,[9]
S-Fe_2O_3	CA	671.02	0.2 - 107	31.25	< 2	This work

Note:

CNPEs: solid carbon nanopipette electrodes.

NSG-Fe_2O_3: both nitrogen and sulfur dual doped graphene supported Fe_2O_3.

ERGO: electrochemically reduced graphene oxide.

Fe_3O_4@GNs: Fe_3O_4@graphene nanospheres.
Fe_3O_4@Au-S-Fc/GS-chitosan: phenylethynyl ferrocene thiolate (Fc-SAc) modified Fe_3O_4@Au NPs coupling with graphene sheet/chitosan (GS-chitosan).
PEDOT/RGO: conducting polymer poly (3,4-ethylenedioxythiophene) (PEDOT) doped with graphene oxide (GO).
GO/SiO_2-MIPs: SiO_2-coated GO and molecularly imprinted polymers.
TENS: self-powered triboelectric nanosensor (TENS) based on the contact-separation mode between a thin layer of poly (tetrafluoroethylene) and an aluminum film.
S-Fe_2O_3: shuttle-like α-Fe_2O_3 NPs.

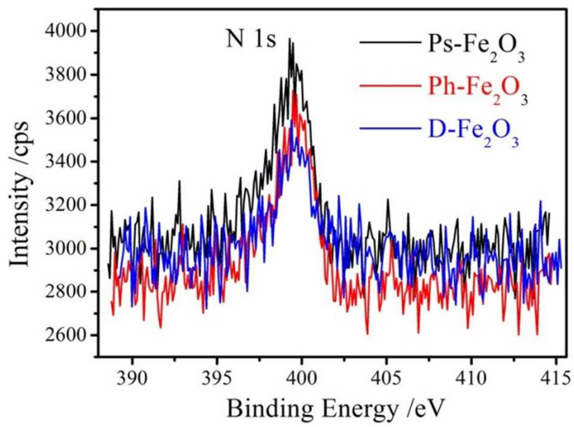

Figure S12. N 1s XPS spectra of the samples: Ps-Fe_2O_3, Ph-Fe_2O_3 and D-Fe_2O_3 without absorbed DA.

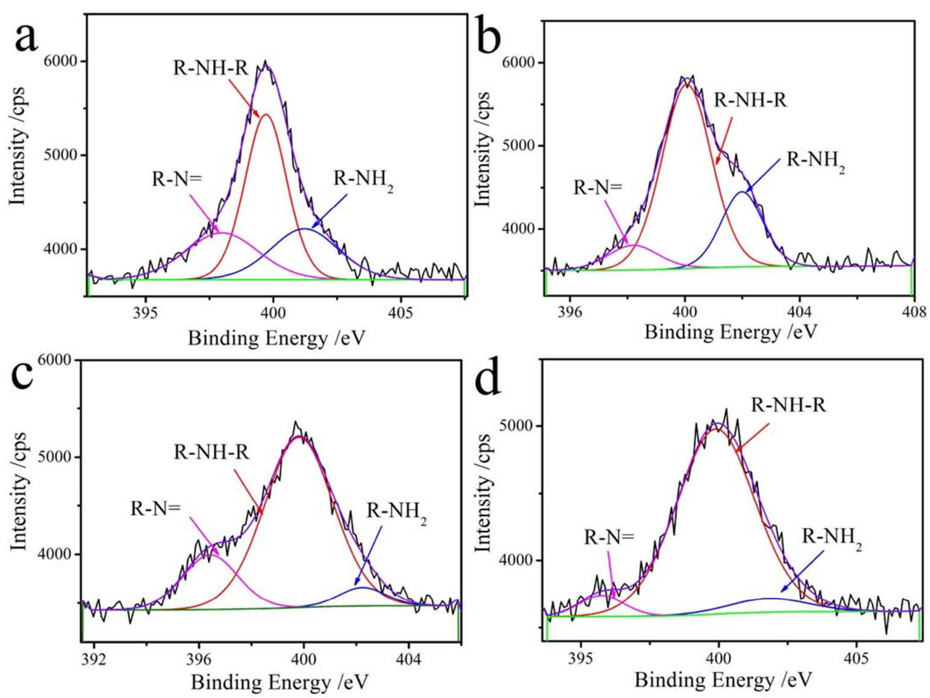

Figure S13. N 1s XPS spectra of the samples: (a) S-Fe_2O_3, (b) Ps-Fe_2O_3, (c) Ph-Fe_2O_3, (d) D-Fe_2O_3 with absorbed DA.

Table S5. Fitting Results of O 1s XPS Spectra of Fe_2O_3 Samples

sample	Oxygen species	Binding energy /eV	Relative percentage /%
	O_L (Fe-O)	529.81	16.85
S-Fe_2O_3	O_V (vacancy)	531.87	33.23
	O_C (chemisorbed)	533.26	49.91
	O_L (Fe-O)	529.72	24.73
Ps-Fe_2O_3	O_V (vacancy)	531.47	30.20
	O_C (chemisorbed)	533.20	45.06
	O_L (Fe-O)	529.73	18.16
Ph-Fe_2O_3	O_V (vacancy)	532.03	50.51
	O_C (chemisorbed)	533.53	31.33
	O_L (Fe-O)	529.85	38.02
D-Fe_2O_3	O_V (vacancy)	531.04	31.10
	O_C (chemisorbed)	532.86	30.88

Table S6. The values of zeta potential of the samples: S-Fe_2O_3, Ps-Fe_2O_3, Ph-Fe_2O_3, D-Fe_2O_3.

sample	Zeta potential	Standard deviation
S-Fe_2O_3	-15.5	0.46
Ps-Fe_2O_3	-12.2	0.36
Ph-Fe_2O_3	-6.35	0.12
D-Fe_2O_3	-3.82	0.15

REFERENCE

(1) Rees, H. R.; Anderson, S. E.; Privman, E.; Bau, H. H.; Venton, B. J. Carbon Nanopipette Electrodes for Dopamine Detection in Drosophila. *Anal. Chem.* **2015**, *87*, 3849–3855.

(2) Yasmin, S.; Ahmed, M. S.; Jeon, S. Determination of Dopamine by Dual Doped Graphene-Fe_2O_3 in Presence of Ascorbic Acid. *J. Electrochem. Soc.* **2015**, *162*, 363–369.

(3) Han, H. S.; Ahmed, M. S.; Jeong, H.; Jeon, S. The Determination of Dopamine in Presence of Serotonin on Dopamine-Functionalized Electrochemically Prepared Graphene Biosensor. *J. Electrochem. Soc.* **2015**, *162*, 75–82.

(4) Zhang, W.; Zheng, J.; Shi, J.; Lin, Z.; Huang, Q.; Zhang, H.; Wei, C.; Chen, J.;

Hu, S.; Hao, A. Nafion Covered Core-Shell Structured Fe_3O_4@graphene Nanospheres Modified Electrode for Highly Selective Detection of Dopamine. *Anal. Chim. Acta* **2015**, *853*, 285–290.

(5) Liu, M.; Chen, Q.; Lai, C.; Zhang, Y.; Deng, J.; Li, H.; Yao, S. A Double Signal Amplification Platform for Ultrasensitive and Simultaneous Detection of Ascorbic Acid, Dopamine, Uric Acid and Acetaminophen Based on a Nanocomposite of Ferrocene Thiolate Stabilized Fe_3O_4@Au Nanoparticles with Graphene Sheet. *Biosens. Bioelectron.* **2013**, *48*, 75–81.

(6) Wang, W.; Xu, G.; Cui, X. T.; Sheng, G.; Luo, X. Enhanced Catalytic and Dopamine Sensing Properties of Electrochemically Reduced Conducting Polymer Nanocomposite Doped with Pure Graphene Oxide. *Biosens. Bioelectron.* **2014**, *58*, 153–156.

(7) Zeng, Y.; Zhou, Y.; Kong, L.; Zhou, T.; Shi, G. A Novel Composite of SiO_2-Coated Graphene Oxide and Molecularly Imprinted Polymers for Electrochemical Sensing Dopamine. *Biosens. Bioelectron.* **2013**, *45*, 25–33.

(8) Jie, Y.; Wang, N.; Cao, X.; Xu, Y.; Li, T.; Zhang, X.; Wang, Z. L. Self-Powered Triboelectric Nanosensor with Poly(tetrafluoroethylene) Nanoparticle Arrays for Dopamine Detection. *ACS Nano* **2015**, *9*, 8376–8383.

(9) Oko, D. N.; Garbarino, S.; Zhang, J.; Xu, Z.; Chaker, M.; Ma, D.; Guay, D.; Tavares, A. C. Dopamine and Ascorbic Acid Electro-Oxidation on Au, AuPt and Pt Nanoparticles Prepared by Pulse Laser Ablation in Water. *Electrochim. Acta* **2015**, *159*, 174–183.